

Synthesis, Evaluation of Antimicrobial Activity, DFT Calculations, and Docking of Some Derivatives of 4-[(1,3,4-Thiadiazol-2-yl)ethenyl]pyrroles

Sergiy Kemskyi ¹ , Alina Grozav ^{2,*} , Vitalii Chornous ² , Nina Yakovychuk ² , Svyatoslav Deyneka ² , Mariana Fedoriv ³ , Dmytro Mel'nyk ³ , Oksana Mel'nyk ³ , Mykhailo Vovk ¹ 

¹ Institute of Organic Chemistry of the National Academy of Sciences of Ukraine, Ukraine

² Bukovinian State Medical University, Ukraine

³ Ivano-Frankivsk National Medical University, Ukraine

* Correspondence: hrozav.alina@bsmu.edu.ua;

Received: 2.06.2024; Accepted: 12.07.2025; Published: 25.11.2025

Abstract: A series of new 4-[(1,3,4-thiadiazol-2-yl)ethenyl]pyrroles has been synthesized by a high-yield reaction between 3-(pyrrole-4-yl)acrylic acids with substituted thiosemicarbazides in boiling POCl₃. The synthesized compounds were identified by IR, NMR, ¹H, ¹³C spectroscopy, mass-spectrometry, and elemental analysis. All synthesized chemicals showed inhibitory activity against some fungi and bacteria. The HOMO-LUMO energies and the molecular electrostatic potentials were calculated for the most active compounds. Additionally, the potential binding affinity of these compounds for the active sites of ThiM *Klebsiella* kinase was evaluated using molecular docking.

Keywords: pyrrole; 1,3,4-thiadiazole; antimicrobial activity; DFT calculation; molecular docking.

© 2025 by the authors. This article is an open-access article distributed under the terms and conditions of the Creative Commons Attribution (CC BY) license (<https://creativecommons.org/licenses/by/4.0/>), which permits unrestricted use, distribution, and reproduction in any medium, provided the original work is properly cited. The authors retain copyright of their work, and no permission is required from the authors or the publisher to reuse or distribute this article, as long as proper attribution is given to the original source.

1. Introduction

Pyrroles with some functional substituents are known as synthetic substrates for various useful compounds. Besides, they are present as key structural elements in some important biomolecules, such as heme, chlorophyll, bile pigments, vitamin B₁₂ [1], sea algae-originated alkaloids [2,3], some widely used remedies: anticancer Sunitinib [4], lipid-lowering Atorvastin [5], anti-inflammatory Tolmetin [6], anti-neurodegenerative Aloracetam [7], and some organic conducting materials [8-10]. As shown in recent investigations, functionalized pyrroles can serve as basic scaffolds for the development of anticancer [11-14], antimicrobial [15-18], and antioxidant drugs [19].

Among other functionally-substituted pyrroles, special attention should be given to the compounds with heteroarylethenyl substituents in the α - or β -positions of the ring. They exhibit antitumor activity [20-22] or can be used as highly effective photocatalysts [23-28], as useful building blocks for the development of antibiotic analogs [29-32], and as polycyclic phosphodiesterase inhibitors [33].

The following structures have been reported as heteroaromatic parts of 1-pyrrolyl-2-heteroarylethenes: pyrrole [26,27,29-31,34], thiophene [24], thiazole [25], imidazoline [21], pyridine [20], benzothiazoline [23], and benzoxazoline [22] rings. In this study, we investigate

a previously unexplored type of ethenylpyrroles, featuring a pharmacophoric 1,3,4-thiadiazole cycle in the vicinal position to the double bond. This cycle, as previously reported, is a key structural component of various bioactive compounds [35-39], the ophthalmologic medicines Acetazolamide and Methazolamide [40], and the antibacterial medicine Megazol [41].

That is why it can be expected that the pharmacophoric pyrrole and 1,3,4-thiadiazole cycles bonded by the ethenyl linker on the same molecular platform should increase their bioactivity. That is why this work aimed to synthesize new derivatives of 4-[(1,3,4-thiadiazol-2-yl)ethenyl]pyrroles, followed by DFT calculations and molecular docking analyses of the most active compounds.

2. Materials and Methods

Compounds **1a-d** were prepared according to [42]. All chemicals were of analytical grade and commercially available. During the synthetic part of the work, reagents from Merck (Germany) and Sigma-Aldrich (USA) were used. All reagents and solvents were used without further purification and drying. All the melting points were determined in an open capillary and left uncorrected. IR spectra were recorded on a Bruker Vertex 70 FT-IR spectrometer for samples in KBr pellets. ¹H-NMR spectra were acquired in pulse Fourier transform mode on a Varian VXR-400 spectrometer (400 MHz) in DMSO-d₆, while ¹³C-NMR spectra of all compounds were recorded on a Bruker Avance DRX-500 spectrometer (125 MHz). Mass spectra were recorded on an Agilent LC/MSD SL mass spectrometer; column: Zorbax SB-C18, 4.6 × 15 mm, 1.8 μm (PN 82 (c)75-932); DMSO solvent, atmospheric pressure electrospray ionization. Elemental analysis was performed on a Perkin Elmer 2400 CHN-analyzer. Melting points were determined on a Kofler bench and left uncorrected.

2.1. General procedure for preparation of compounds 3a-j.

A mixture of 5 mmol of the acids 1a-d, 5 mmol of a mono- or disubstituted thiosemicarbazide 2a-h, and phosphorus oxychloride (2.30 g, 15 mmol) was boiled for 2 h and then cooled to room temperature. Then, some ice was added to the mixture before it was neutralized with a solution of ammonium hydroxide. The obtained solid product was filtered, rinsed with water, dried, and recrystallized from acetonitrile.

2.1.1. Ethyl 4-[2-(5-anilino-1,3,4-thiadiazol-2-yl)vinyl]-5-chloro-1,2-dimethyl-1*H*-pyrrole-3-carboxylate (3a).

Yield 1.612 g (80%); mp 240-241°C. IR (KBr), ν_{\max} (cm⁻¹): 1637 (C=C), 1719 (C=O), 3272 (N-H). ¹H-NMR (400 MHz; DMSO-d₆, ppm): δ 1.31 (t, $J = 7.2$ Hz, 3H, OCH₂CH₃), 2.45 (s, 3H, CH₃), 3.49 (s, 3H, NCH₃), 4.20 (q, $J = 7.0$ Hz, 2H, OCH₂CH₃), 6.98 (t, $J = 7.1$ Hz, 1H, Ar), 7.25 (d, $J = 16.7$ Hz, 1H, CH=CH), 7.32 (t, $J = 7.6$ Hz, 2H, Ar), 7.49 (d, $J = 16.7$ Hz, 1H, CH=CH), 7.64 (d, $J = 7.8$ Hz, 2H, Ar), 10.60 (s, 1H, NH). ¹³C-NMR (126 MHz; DMSO-d₆, ppm): δ 12.3, 14.7, 31.4, 60.0, 109.7, 115.1, 115.8, 117.9 (2C), 118.8, 122.4, 128.5, 129.5 (2C), 137.3, 141.0, 159.3, 162.7, 164.4. HR-ESI-MS: m/z 403 [M+H]⁺ (calcd. 402.91 for C₁₉H₁₉ClN₄O₂S); Anal. calcd. for C₁₉H₁₉ClN₄O₂S: C, 56.64; H, 4.75; N, 13.91; S, 7.96. Found: C, 56.49; H, 4.66; N, 14.05; S, 8.14.

2.1.2. Ethyl 5-chloro-4-(2-{5-[(4-methoxyphenyl)amino]-1,3,4-thiadiazol-2-yl}vinyl)-1,2-dimethyl-1*H*-pyrrole-3-carboxylate (3b).

Yield 1.556 g (72%); mp 180-181°C. IR (KBr), ν_{\max} (cm⁻¹): 1642 (C=C), 1714 (C=O), 3281 (N-H). ¹H-NMR (400 MHz; DMSO-*d*₆, ppm): δ 1.32 (t, *J* = 7.2 Hz, 3H, OCH₂CH₃), 2.48 (s, 3H, CH₃), 3.53 (s, 3H, NCH₃), 3.74 (s, 3H, OCH₃), 4.22 (q, *J* = 7.2 Hz, 2H, OCH₂CH₃), 6.94 (d, *J* = 8.8 Hz, 2H, Ar), 7.27 (d, *J* = 16.7 Hz, 1H, CH=CH), 7.50 (d, *J* = 16.7 Hz, 1H, CH=CH), 7.57 (d, *J* = 8.8 Hz, 2H, Ar), 11.53 (s, 1H, NH). ¹³C-NMR (126 MHz; DMSO-*d*₆, ppm): δ 11.8, 14.2, 30.9, 55.2, 59.5, 109.2, 114.2 (2C), 114.5, 115.5, 117.8, 119.7 (2C), 128.3, 133.7, 136.9, 154.8, 158.2, 162.9, 163.9. HR-ESI-MS: *m/z* 433 [M+H]⁺ (calcd. 432.93 for C₂₀H₂₁ClN₄O₃S); Anal. calcd. for C₂₀H₂₁ClN₄O₃S: C, 55.49; H, 4.89; N, 12.94; S, 7.41. Found: C, 55.69; H, 4.86; N, 13.05; S, 7.53.

2.1.3. Ethyl 5-chloro-4-{2-[5-(dimethylamino)-1,3,4-thiadiazol-2-yl]vinyl}-1,2-dimethyl-1*H*-pyrrole-3-carboxylate (3c).

Yield 1.242 g (70%); mp 150-151°C. IR (KBr), ν_{\max} (cm⁻¹): 1647 (C=C), 1712 (C=O). ¹H-NMR (400 MHz; DMSO-*d*₆, ppm): δ 1.32 (t, *J* = 7.2 Hz, 3H, OCH₂CH₃), 2.48 (s, 3H, CH₃), 3.11 (s, 6H, 2NCH₃), 3.53 (s, 3H, NCH₃), 4.22 (q, *J* = 7.2 Hz, 2H, OCH₂CH₃), 7.23 (d, *J* = 16.7 Hz, 1H, CH=CH), 7.42 (d, *J* = 16.7 Hz, 1H, CH=CH). ¹³C-NMR (126 MHz; DMSO-*d*₆, ppm): δ 11.9, 14.2, 30.9, 41.0 (2C), 59.5, 109.1, 114.7, 115.0, 118.8, 126.4, 136.6, 157.9, 164.0, 169.5. HR-ESI-MS: *m/z* 355 [M+H]⁺ (calcd. 354.86 for C₁₅H₁₉ClN₄O₂S); Anal. calcd. for C₁₅H₁₉ClN₄O₂S: C, 50.77; H, 5.40; N, 15.79; S, 9.04. Found: C, 50.49; H, 5.49; N, 15.60; S, 8.90.

2.1.4. Ethyl 5-chloro-4-{2-[5-(cyclohexylamino)-1,3,4-thiadiazol-2-yl]vinyl}-2-methyl-1-propyl-1*H*-pyrrole-3-carboxylate (3d).

Yield 1.704 g (78%), mp 185-186°C. IR(KBr), ν_{\max} (cm⁻¹): 1634 (C=C), 1714 (C=O), 3287 (N-H). ¹H-NMR (400 MHz, DMSO-*d*₆ ppm): δ 0.88 (t, *J* = 7.2 Hz, 3H, NCH₂CH₂CH₃), 1.14-1.33 (m, 8H, OCH₂CH₃+ NCH₂CH₂CH₃+cyclohexyl), 1.53-1.73 (m, 5H, cyclohexyl), 1.91-2.01 (m, 2H, cyclohexyl), 3.52-3.56 (m, 1H, cyclohexyl), 3.93 (t, *J* = 7.2 Hz, 2H, NCH₂CH₂CH₃), 4.21 (q, *J* = 7.2 Hz, 2H, OCH₂CH₃), 7.19 (d, *J* = 16.7 Hz, 1H, CH=CH), 7.33 (d, *J* = 16.7 Hz, 1H, CH=CH), 7.81-7.91 (m, 1H). ¹³C-NMR (126 MHz; DMSO-*d*₆, ppm): δ 10.7, 11.7, 14.2, 22.6, 24.3 (2C), 25.2, 32.0 (2C), 45.2, 53.6, 59.5, 109.5, 114.4, 115.0, 119.3, 126.3, 136.2, 156.8, 163.9, 165.9. HR-ESI-MS: *m/z* 438 [M+H]⁺ (calcd. 437.01 for C₂₁H₂₉ClN₄O₂S); Anal. calcd. for C₂₁H₂₉ClN₄O₂S: C, 57.72; H, 6.69; N, 12.82; S, 7.34. Found: C, 57.37; H, 6.80; N, 12.70; S, 7.24.

2.1.5. Ethyl 4-[-2-(5-anilino-1,3,4-thiadiazol-2-yl)vinyl]-5-chloro-2-methyl-1-propyl-1*H*-pyrrole-3-carboxylate (3e).

Yield 1.724 g (80%); mp 183-184°C. IR (KBr), ν_{\max} (cm⁻¹): 1640 (C=C), 1720 (C=O), 3274 (N-H). ¹H-NMR (400 MHz; DMSO-*d*₆, ppm): δ 0.93 (t, *J* = 7.3 Hz, 3H, NCH₂CH₂CH₃), 1.10 (t, *J* = 7.1 Hz, 3H, OCH₂CH₃), 1.29 - 1.39 (m, 2H, NCH₂CH₂CH₃), 2.53 (s, 3H, CH₃), 4.00 (t, *J* = 7.2 Hz, 2H, NCH₂CH₂CH₃), 4.08 (q, *J* = 7.0 Hz, 2H, OCH₂CH₃), 7.00 (t, *J* = 7.3 Hz, 1H, Ar), 7.27 (d, *J* = 16.7 Hz, 1H, CH=CH), 7.35 (t, *J* = 7.9 Hz, 2H, Ar), 7.49 (d, *J* = 16.7 Hz, 1H, CH=CH), 7.64 (t, *J* = 7.8 Hz, 2H, Ar), 10.36 (s, 1H, NH). ¹³C-NMR (126 MHz; DMSO-*d*₆, ppm): δ 11.2, 13.5, 13.9, 19.2, 43.9, 59.4, 109.6, 110.9, 112.8, 116.7, 117.2 (2 C),

121.7, 129.0 (2C), 133.8, 135.6, 140.6, 149.5, 163.1, 165.0. HR-ESI-MS: m/z 431 $[M+H]^+$ (calcd. 430.96 for $C_{21}H_{23}ClN_4O_2S$); Anal. calcd. for $C_{21}H_{23}ClN_4O_2S$: C, 58.53; H, 5.38; N, 13.00; S, 7.44. Found: C, 58.29; H, 5.46; N, 12.85; S, 7.60.

2.1.6. Ethyl 5-chloro-4-(2-{5-[(4-fluorophenyl)amino]-1,3,4-thiadiazol-2-yl}vinyl)-2-methyl-1-propyl-1*H*-pyrrole-3-carboxylate (3f).

Yield 1.616 g (72%); mp 218-219°C, IR (KBr), ν_{max} (cm^{-1}): 1644 (C=C), 1718 (C=O), 3270 (N-H). 1H -NMR (400 MHz; DMSO- d_6 , ppm): δ 0.88 (t, $J = 7.2$ Hz, 3H, $NCH_2CH_2CH_3$), 1.32 (t, $J = 7.2$ Hz, 3H, OCH_2CH_3), 1.59-1.68 (m, 2H, $NCH_2CH_2CH_3$), 3.94 (t, $J = 7.0$ Hz, 3H, $NCH_2CH_2CH_3$), 4.22 (q, $J = 7.2$ Hz, 2H, OCH_2CH_3), 7.18 (t, $J = 8.5$ Hz, 2H, Ar), 7.27 (d, $J = 16.7$ Hz, 1H, CH=CH), 7.49 (d, $J = 16.7$ Hz, 1H, CH=CH), 7.64-7.67 (m, 2H, Ar), 10.50 (s, 1H, NH). ^{13}C -NMR (126 MHz; DMSO- d_6 , ppm): δ 10.7, 11.7, 14.2, 22.6, 45.2, 59.6, 109.6, 114.8, 114.9, 115.5, 115.7 (d, $J^1 = 6.3$ Hz, 2C), 118.4, 119.2, 119.2, 128.1 (d, $J^2 = 21.7$ Hz, 2C), 136.4, 136.9, 158.7, 162.4 (d, $J^3 = 245.2$, C-F, Hz). HR-ESI-MS: m/z 449 $[M+H]^+$ (calcd. 448.95 for $C_{21}H_{22}ClFN_4O_2S$); Anal. calcd. for $C_{21}H_{22}ClFN_4O_2S$: C, 56.18; H, 4.94; N, 12.48; S, 7.14. Found: C, 56.36; H, 5.06; N, 12.35; S, 7.30.

2.1.7. Ethyl 1-butyl-5-chloro-4-{2-[5-(cyclohexylamino)-1,3,4-thiadiazol-2-yl]vinyl}-2-methyl-1*H*-pyrrole-3-carboxylate (3g).

Yield 1.759 g (78%); mp 135-136°C. IR (KBr), ν_{max} (cm^{-1}): 1638 (C=C), 1716 (C=O), 3285 (N-H). 1H -NMR (400 MHz, DMSO- d_6 ppm): δ 0.92 (t, $J = 7.2$ Hz, 3H, $NCH_2CH_2CH_2CH_3$), 1.18-1.37 (m, 10H, $NCH_2CH_2CH_2CH_3+OCH_2CH_3+cyclohexyl$), 1.56-1.78 (m, 5H, $NCH_2CH_2CH_2CH_3+cyclohexyl$), 1.92-2.04 (m, 2H, cyclohexyl), 2.50 (s, 3H, CH_3), 3.48-3.58 (m, 1H, cyclohexyl), 3.97 (t, $J = 7.2$ Hz, 2H, $NCH_2CH_2CH_2CH_3$), 4.22 (q, $J = 7.2$ Hz, 2H, OCH_2CH_3), 7.20 (d, $J = 16.7$ Hz, 1H, CH=CH), 7.33 (d, $J = 16.7$ Hz, 1H, CH=CH), 7.74 – 7.77 (m, 1H). ^{13}C -NMR (126 MHz; DMSO- d_6 , ppm): δ 11.7, 13.4, 14.2, 19.2, 24.3, 25.2 (2C), 31.4, 32.0 (2C), 43.6, 45.2, 53.6, 59.5, 109.5, 114.4, 115.0, 119.3, 126.3, 136.2, 156.8, 163.9, 165.9. HR-ESI-MS: m/z 452 $[M+H]^+$ (calcd. 451.03 for $C_{22}H_{31}ClN_4O_2S$); Anal. calcd. for $C_{22}H_{31}ClN_4O_2S$: C, 58.59; H, 6.93; N, 12.42; S, 7.11. Found: C, 58.80; H, 7.00; N, 12.60; S, 7.00.

2.1.8. Ethyl 1-butyl-5-chloro-2-methyl-4-[2-(5-morpholin-4-yl-1,3,4-thiadiazol-2-yl)vinyl]-1*H*-pyrrole-3-carboxylate (3h).

Yield 1.536 g (70%), mp 120-121°C. IR (KBr), ν_{max} (cm^{-1}): 1642 (C=C), 1714 (C=O). 1H -NMR (400 MHz; DMSO- d_6 , ppm): δ 1H NMR (400 MHz, DMSO- d_6) δ 0.91 (t, $J = 7.2$ Hz, 3H, $NCH_2CH_2CH_2CH_3$), 1.29-1.35 (m, 5H, $NCH_2CH_2CH_2CH_3+OCH_2CH_3$), 1.55-1.63 (m, 2H, $NCH_2CH_2CH_2CH_3$), 2.51 (s, 3H, CH_3), 3.47 (br.s, 4H, morpholin), 3.73 (br.s, 4H, morpholin), 3.97 (t, $J = 7.2$ Hz, 2H, $NCH_2CH_2CH_2CH_3$), 4.22 (q, $J = 7.0$ Hz, 2H, OCH_2CH_3), 7.25 (d, $J = 16.7$ Hz, 1H, CH=CH), 7.46 (d, $J = 16.7$ Hz, 1H, CH=CH). ^{13}C -NMR (126 MHz; DMSO- d_6 , ppm): δ 11.70, 13.47, 14.18, 19.22, 31.34, 40.37, 43.60, 49.39 (2C), 59.53, 65.2 (2C), 109.54, 114.89, 118.64, 127.1, 136.11, 158.79, 163.94, 170.11. HR-ESI-MS: m/z 439 $[M+H]^+$ (calcd. 438.98 for $C_{20}H_{27}ClN_4O_3S$); Anal. calcd. for $C_{20}H_{27}ClN_4O_3S$: C, 54.72; H, 6.20; N, 12.76; S, 7.30. Found: C, 54.90; H, 6.08; N, 12.60; S, 7.20.

2.1.9. Ethyl 1-butyl-5-chloro-2-methyl-4-(2-{5-[(4-methylphenyl)amino]-1,3,4-thiadiazol-2-yl}vinyl)-1*H*-pyrrole-3-carboxylate (3i).

Yield 1.616 g (72%), mp 218-219°C. IR (KBr), ν_{\max} (cm⁻¹): 1644 (C=C), 1720 (C=O), 3280 (N-H). ¹H-NMR (400 MHz; DMSO-d₆, ppm): δ 0.91 (t, $J = 7.2$ Hz, 3H, NCH₂CH₂CH₂CH₃), 1.29-1.36 (m, 5H, NCH₂CH₂CH₂CH₃+OCH₂CH₃), 1.52-1.65 (m, 2H, NCH₂CH₂CH₂CH₃), 2.26 (s, 3H, 3CH₃), 3.96 (t, $J = 7.0$ Hz, 2H, NCH₂CH₂CH₂CH₃), 4.23 (q, $J = 7.0$ Hz, 2H, OCH₂CH₃), 7.15 (d, $J = 7.8$ Hz, 2H, Ar), 7.28 (d, $J = 16.7$ Hz, 1H, CH=CH), 7.45 – 7.58 (m, 3H, CH=CH + Ar), 10.46 (s, 1H, NH). ¹³C-NMR (126 MHz; DMSO-d₆, ppm): δ 11.7, 13.5, 14.2, 19.2, 20.3, 31.3, 43.6, 59.6, 109.6, 114.8, 117.7 (2C), 118.4, 127.9, 128.5, 128.9, 129.4 (2C), 131.0, 136.2, 138.0, 162.5, 163.9. HR-ESI-MS: m/z 460 [M+H]⁺ (calcd. 459.01 for C₂₃H₂₇ClN₄O₂S); Anal. calcd. for C₂₃H₂₇ClN₄O₂S: C, 60.18; H, 5.93; N, 12.21; S, 6.99. Found: C, 59.94; H, 6.02; N, 12.35; S, 7.10.

2.1.10. Ethyl 1-benzyl-4-[2-(5-anilino-1,3,4-thiadiazol-2-yl)vinyl]-5-chloro-2-methyl-1*H*-pyrrole-3-carboxylate (3j).

Yield 1.964 g (82%); mp 199-200°C. IR (KBr), ν_{\max} (cm⁻¹): 1646 (C=C), 1716 (C=O), 3283 (N-H). ¹H-NMR (400 MHz; DMSO-d₆, ppm): δ 1.35 (t, $J = 7.2$ Hz, 3H, OCH₂CH₃), 2.45 (s, 3H, CH₃), 4.18-4.39 (m, 2H, OCH₂CH₃), 5.34 (s, 2H, CH₂Ph), 7.03 (d, $J = 7.4$ Hz, 3H, Ar), 7.30-7.40 (m, 6H, CH=CH + Ar), 7.57 (d, $J = 16.7$ Hz, 1H, CH=CH), 7.65 (d, $J = 7.9$ Hz, 2H, Ar), 10.48 (s, 1H, NH). ¹³C-NMR (126 MHz; DMSO-d₆, ppm): δ 11.8, 14.2, 46.8, 59.7, 110.1, 115.2, 115.5, 117.5 (2C), 118.8, 122.0, 125.8 (2C), 127.5, 127.9, 128.9 (2C), 129.1 (2C), 136.0, 136.8, 140.4, 158.6, 162.4, 163.9. HR-ESI-MS: m/z 480 [M+H]⁺ (calcd. 479.00 for C₂₅H₂₃ClN₄O₂S); Anal. calcd. for C₂₅H₂₃ClN₄O₂S: C, 62.69; H, 4.84; N, 11.70; S, 6.69. Found: C, 62.84; H, 4.72; N, 11.85; S, 6.80.

2.2. Antimicrobial activities.

The antimicrobial activity of the synthesized compounds was investigated using the nutrient broth microdilution method, as recommended by EUCAST (European Committee on Antimicrobial Susceptibility Testing) [43]. According to this method, the minimal inhibitory concentration (MIC) was determined as the concentration of every synthesized compound required to suppress the proliferation of the given microbial culture in the multihole microplate. The stock 1000 μ g/mL solution was prepared by dissolving the required amount of the compound in dimethyl sulfoxide (DMSO). Further, diluted solutions with concentrations from 500 to 3.9 μ g/mL (or from 500 to 0.48 μ g/mL in the case of control drugs) were used to find the MIC values. The sensitivity of every microbial culture to every concentration of the synthesized compounds was tested three times. Besides, control experiments were carried out to assess the proliferation of microbes in clean broth, in the same broth with an admixture of DMSO, and in the broth with DMSO and the control drugs (Decasanum [44] and Clotrimazole [45]) (Table 2). The control clear broth remained sterile and transparent (no proliferation of the microbial cultures), while some proliferation of the cultures was observed in the case of a mixture of DMSO and the broth.

2.3. Computational analyses.

The software Gaussian09 [46] was employed to optimize the structures of the most active antimicrobial compounds 3c, e, g, and j, and GaussView 5.0.8 was used to visualize the

optimization results. To optimize the geometric structures of the synthesized antimicrobial agents, Density Functional Theory (DFT) was used with the B3LYP functional and the 6-311++G(d,p) basis set.

The following parameters of reactivity were calculated from the ionization potential (IP) and electron affinity (EA) for the compounds **3c**, **e**, **g**, **j**: chemical hardness (η), electron donating power (ω^-), and electron acceptor power (ω^+). IP and EA were calculated by the equations:

$$\text{IP} = -E_{\text{HOMO}} \quad (1)$$

$$\text{EA} = -E_{\text{LUMO}} \quad (2)$$

The chemical hardness (η), electron-donating power (ω^-), and electron acceptor power (ω^+) properties were calculated by the equations [47]:

$$\eta = 0,5(\text{IP} - \text{EA}) \quad (3)$$

$$\text{DEL!} (\omega^- = \frac{(3\text{IP} + \text{EA})^2}{16(\text{IP} - \text{EA})}) \quad \omega = \frac{(3\text{IP} + \text{EA})^2}{16(\text{IP} - \text{EA})} \quad (4)$$

$$\text{DEL!} (\omega^+ = \frac{(\text{IP} + 3\text{EA})^2}{16(\text{IP} - \text{EA})}) \quad \omega = \frac{(\text{IP} + 3\text{EA})^2}{16(\text{IP} - \text{EA})} \quad (5)$$

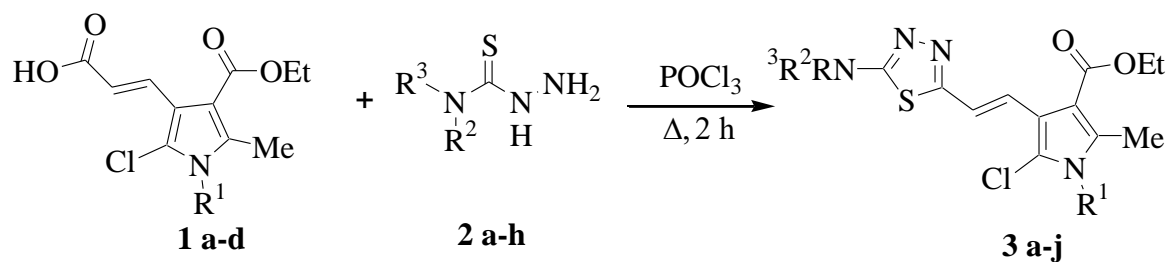
2.4. Molecular docking analysis procedure.

The molecular docking study was performed using the software Autodock Vina [48]. The preliminary optimized structures (B3LYP/6-311++G(d,p)) were used in all our calculations. The crystal structure of kinase ThiM *Klebsiella pneumoniae* was downloaded from the Protein Data Bank (PDB 6k28), the water molecules were removed, the polar hydrogen atoms and the Gasteiger charges were added to the protein structure. The C chain of the protein was also removed, as the investigated docking site lies between chains A and B. A center of the ligand docking cavity (21.0; 62.4; 37.2) was determined using BIOVIA Discovery Studio Visualizer v21.1. The cavity dimension was 20 x 20 x 20. The docking was visualized using BIOVIA Discovery Studio Visualizer v21.1.

3. Results and Discussion

3.1. Chemistry.

3-(Pyrrole-4-yl)acrylic acids **1a-d** with an additional functionalization of the pyrrole ring by a biophoric atom of chlorine [49, 50] and the ester fragment, which is convenient for further modification, were used as substrates for the transformation into ethenes with the vicinal substitution by the pyrrole and 1,3,4-thiadiazole cycles. Postfunctionalization of their carboxylic groups by N-substituted thiosemicarbazides **2a-h** in excessive boiling POCl₃, according to [51], showed a high efficiency in the formation of a 5-amino-1,3,4-thiadiazole cycle of the target compounds **3a-j** (see Scheme 1). It should be emphasized that under the conditions reported in [51], this process runs regioselectively, and no alternative 1,3,4-triazole-2-thiones [52] or 1,3,4-oxodiazoles [53] are formed.



1, R¹ = Me (a), Pr (b), Bu (c), PhCH₂ (d);

2, R² = H, R³ = Me (a); R² = H, R³ = cyclo C₆H₁₁ (b); R² = H, R³ = Ph (c);

R² = H, R³ = 4-FC₆H₄ (d); R² = H, R³ = 4-MeC₆H₄ (e);

R² = H, R³ = 4-MeOC₆H₄ (f); R² = R³ = Me (g); R² R³ = (CH₂)₂O(CH₂)₂ (h)

Scheme 1. Synthesis of new derivatives of 4-[(1,3,4-thiadiazol-2-yl)ethenyl]pyrroles **3a-j**.

Table 1. Structure of synthesized compounds.

No	Structure	No	Structure
3a		3f	
3b		3g	
3c		3h	
3d		3i	
3e		3j	

The structures of all synthesized compounds (Table 1) were studied by IR, ¹H NMR, ¹³C NMR, mass spectrometry, and elemental analysis (see Experimental above). The IR absorption bands at 1634-1647 and 1710-1720 cm⁻¹ were attributed to the valence oscillations of C=C and C=O bonds, respectively. The N-H bonds of compounds **3a, b, d-g, i, j** reveal their absorption bands within 3272-3287 cm⁻¹. Regarding the ¹H NMR spectra, they reveal the peaks related to the substituents of both heterocyclic rings together with the characteristic doublets of the ethenyl fragment's protons, ranging between 7.19-7.40 and 7.33-7.57 ppm with a spin-spin constant of 16.7 Hz. It proves a *trans*-configuration of the pyrrole and 1,3,4-thiadiazole cycles in the molecules **3a-j**. The N-H protons of arylamino groups of **3a, b, e, f, i, j** are

attributed to the singlets ranging between 10.46 and 11.53 ppm. On the contrary, their N-alkyl analogs **3d** and **g** do not show such signals, which, perhaps, is caused by the exchange of the N-H protons with the deuterium solvent's water molecules.

3.2. Antimicrobial activity.

Synthesized 4-[(1,3,4-thiadiazol-2-yl)ethenyl]pyrroles **3a-j** exhibit antibacterial and antifungal activity against some bacterial (*Escherichia coli* ATCC 25922, *Klebsiella pneumonia* ATCC 1388, *Pseudomonas aeruginosa* ATCC 27853, *Proteus vulgaris* 4636, and *Staphylococcus aureus* ATCC 25923) and fungal (*Aspergillus niger* K9 and *Candida albicans* ATCC 885/653) test-strains. For these compounds, MICs range from 31.25 to 125 µg/mL, while their minimal bactericidal (fungicidal) concentrations range from 62.5 to 250 µg/mL (Tables 2, 3).

Table 2. Antibacterial activity of new derivatives of 4-[(1,3,4-thiadiazol-2-yl)ethenyl]pyrroles **3 a-j**.

No	<i>K. pneumoniae</i>		<i>S. aureus</i>		<i>E. coli</i>		<i>P. vulgaris</i>		<i>P. aeruginosa</i>	
	MIC	MBC	MIC	MBC	MIC	MBC	MIC	MBC	MIC	MBC
3a	62.5	62.5	125	250	62.5	62.5	125	125	62.5	62.5
3b	62.5	125	125	250	125	250	125	250	62.5	62.5
3c	31.25	62.5	125	250	62.5	62.5	125	125	31.25	62.5
3d	62.5	62.5	125	125	62.5	62.5	125	125	31.25	62.5
3e	31.25	62.5	62.5	125	31.25	62.5	62.5	62.5	31.25	62.5
3f	62.5	62.5	125	250	125	125	125	125	31.25	62.5
3g	31.25	62.5	62.5	62.5	31.25	62.5	62.5	62.5	62.5	125
3h	62.5	62.5	125	125	62.5	62.5	125	125	62.5	62.5
3i	62.5	125	125	250	62.5	125	125	125	31.25	62.5
3j	31.25	62.5	62.5	125	31.25	62.5	31.25	62.5	31.25	125
DMSO*	+		+		+		+		+	
C**	15.625	31.25	0.48	0.97	1.95	3.9	7.81	15.625	31.25	31.25

* proliferation of bacteria detected; ** Decasan (a solution consisting of 0.2 mg/mL of decamethoxin) made by “Yuria-Pharm” was used as the control drug.

Table 3. Antifungal activity of new derivatives of 4-[(1,3,4-thiadiazol-2-yl)ethenyl]pyrroles **3 a-j**.

No	<i>C. albicans</i>		<i>A. niger</i>	
	MIC	MFC	MIC	MFC
3a	62.5	62.5	62.5	125
3b	62.5	62.5	62.5	125
3c	62.5	62.5	62.5	125
3d	62.5	62.5	62.5	125
3e	62.5	62.5	62.5	125
3f	62.5	62.5	62.5	125
3g	62.5	62.5	62.5	125
3h	62.5	62.5	62.5	125
3i	62.5	62.5	62.5	125
3j	62.5	62.5	62.5	125
DMSO*	+		+	
C**	0.97	1.95	0.48	0.48

* proliferation of bacteria detected; ** Clotrimazole (a solution consisting of 10 mg/mL of clotrimazole) made by PJSC SIC “Borshchahivskiy CPP” was used as the control drug.

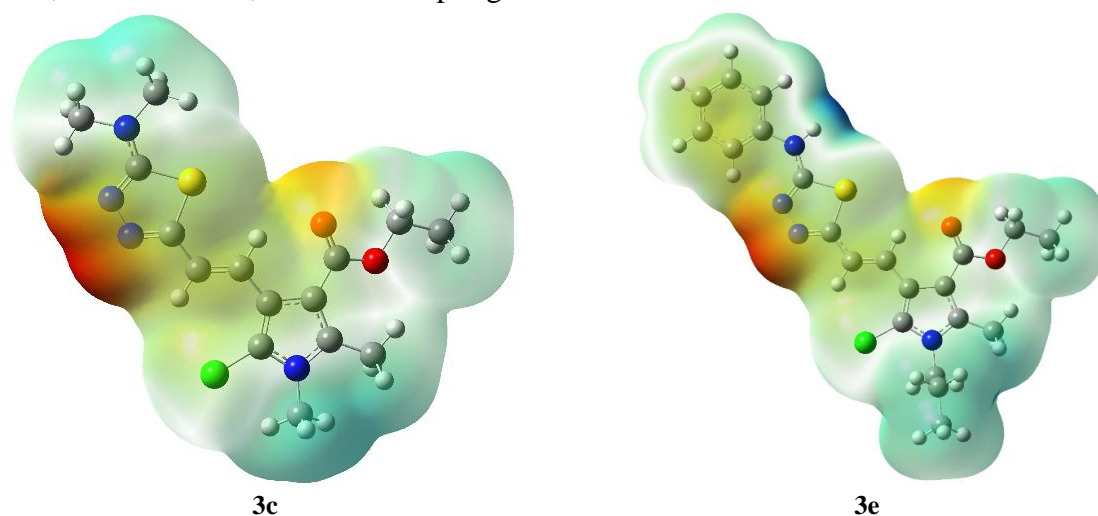
Specific antistaphylococcus activity against the test-strain *Staphylococcus aureus* ATCC 25923 is moderate with a MIC of 62.5 or 125 µg/mL. The highest antimicrobial activity was observed for compounds **3e**, **3g**, and **3j**, with a MIC of 31.25 µg/mL for **3j** against the enterobacterium *Proteus vulgaris* 4636. It should be noted that a concentration of 31.25 µg/mL of **3e**, **3g**, **3j** is sufficient to inhibit the proliferation of the gram-negative bacteria *Escherichia*

coli ATCC 25922. Another antibacterial study was conducted on the test strain, *Pseudomonas aeruginosa* ATCC 27853, since this microorganism causes severe acute and chronic diseases in patients with weakened immunity. Besides, this microbe is quite antibiotic-resistant due to its biofilm-forming ability [54]. The highest activity against *Pseudomonas aeruginosa* ATCC 27853 was found for the compounds **3c**, **d-f**, **3i**, **3j** (MIC=31.25 µg/mL). The study of the antibacterial activity against *Klebsiella pneumoniae* ATCC 1388 is also of high interest, as this organism is one of the most common pathogens of pneumonia, urinary tract infections, and bacteremia [55]. In this context, the highest activity was found for **3c**, **3e**, **3g**, **3j**. The activity against fungi *Aspergillus niger* K9 and *Candida albicans* ATCC 885/653 is not selective, and the minimal inhibitory concentration of the entire series of synthesized compounds is 62.5 µg/mL. In the case of *Candida albicans* ATCC 885/653, this content corresponds to the fungicidal concentration.

3.3. Computational analyses.

3.3.1. MEP analysis.

The molecular electrostatic surface potential (MESP) is an important factor for describing the active sites of ligands [56, 57]. For the most active **3c**, **e**, **g**, **j** molecules of *Klebsiella pneumoniae* ATCC 1388, optimised structures were used with the B3LYP/6-311++G(d,p) basis to study the nucleophilic and electrophilic regions on the ligand surface. Fig. 1 shows the presence of two positive regions (nucleophilic site): a small one located on the NH group and more positively charged, and a larger, but less positively charged one located on the alkyl substituents of the pyrrole ring. The presence of phenyl groups in the structures of compounds **3e**, **j** increases the positive charge on the amino group, whereas electron-donating aliphatic substituents in compounds **3c**, **g** decrease it. One of the negatively charged regions (electrophilic site) is located above the nitrogen atoms of the 1,3,4-thiadiazole fragment (more negatively charged), and the other is near the oxygen atom of the ester group (less negatively charged). Nonaromatic electron-donating substituents increase the negative charge in these regions, and vice versa, electron-accepting aromatic substituents decrease it.



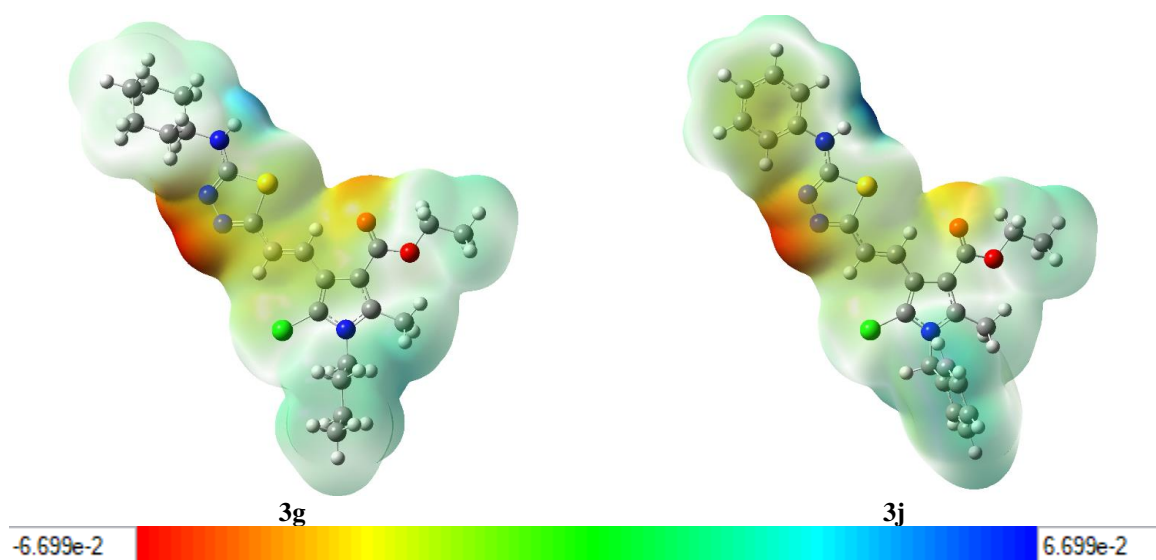


Figure 1. Calculated MESP of compounds **3c,e,g,j** (For comparison, the colour range for all molecules was set from red at -0.06699 a.u. (-42.0 kcal/mol) to blue at +0.06699 a.u. (+42.0 kcal/mol)).

3.3.2. Frontier molecular orbital analysis.

The distribution of the boundary orbitals (Figure 2) shows that both HOMO and LUMO are distributed throughout the conjugated system, which lies almost in the same plane. LUMO is less concentrated on the amino aryl substituent (compounds **3e** and **3j**) and the nitrogen atom at position 4 of the thiadiazole ring, but extends to the carboxylate group. Whereas HOMO completely covers the aminoaryl substituent (compounds **3e** and **3j**) and is absent on the sulphur atom of the thiazole ring and the carboxylate group.

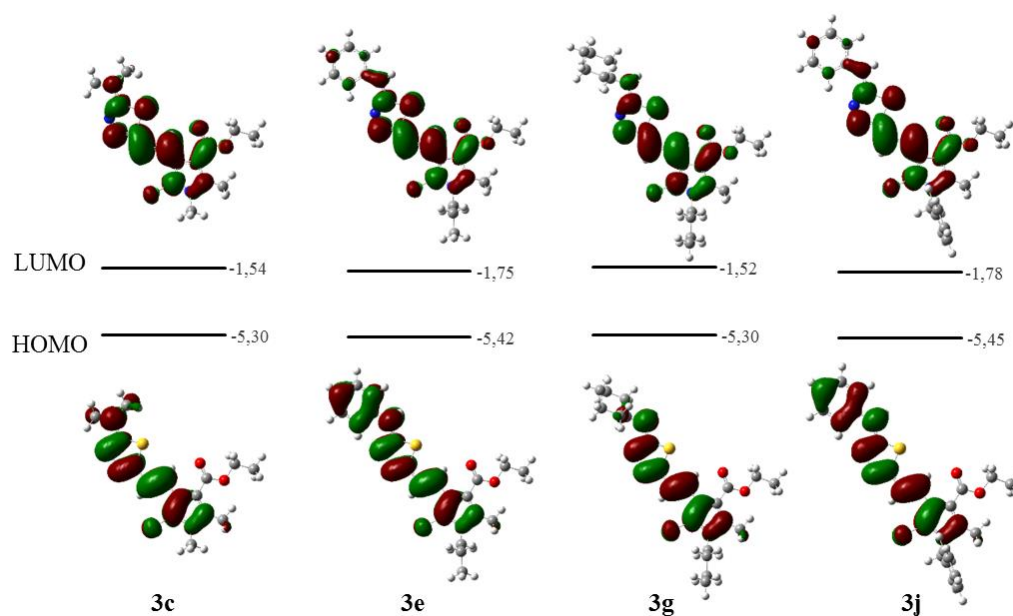


Figure 2. The HOMO and LOMO distributions of **3c, 3e, 3g** and **3j** molecules

The energy of the frontier molecular orbitals is almost the same, but the smaller conjugated system of compounds **3c,g** leads to a slight increase in the energy gap (E_g). In addition, the amino aryl group of compounds **3e, j** reduces the energy of both frontier orbitals, and the less donor benzyl substituent in compound **3j** contributes to this even more. Table 4

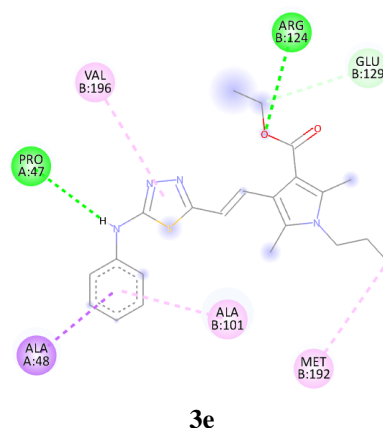
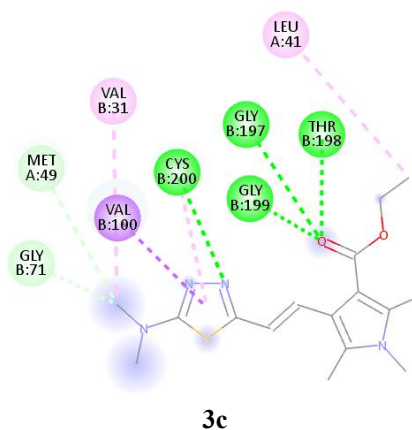
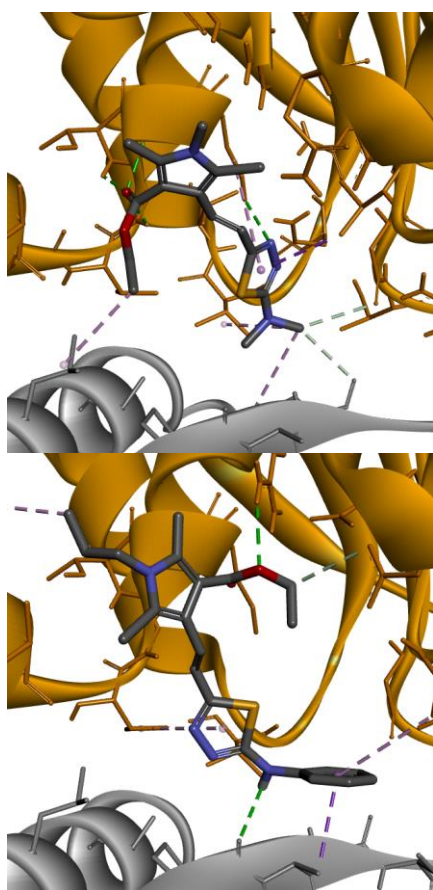
shows the calculated HOMO, LUMO, and energy gap values for the studied compounds. The calculated HOMO energies showed that the values can be ordered as **3c** = **3g** > **3e** > **3j**.

Table 4. The HOMO-LUMO energies and related parameters of compounds **3c**, **3e**, **3g** and **3j**.

	3c	3e	3g	3j
E _{HOMO} , eB	-1,54	-1,75	-1,52	-1,78
E _{LUMO} , eB	-5,30	-5,42	-5,30	-5,45
E _g , eB	3,75	3,68	3,77	3,67
IP, eB	5,30	5,42	5,30	5,45
EA, eB	1,54	1,75	1,52	1,78
η, eB	1,88	1,84	1,89	1,83
ω ⁻ , eB	5,06	5,52	5,02	5,60
ω ⁺ , eB	1,64	1,93	1,61	1,99

3.3.3. Molecular docking analysis.

The molecular docking results were reported as 9 positions per ligand, along with the corresponding ligand-protein binding affinities. The best ligand-protein binding results were: -6.9, -7.2, -7.4, and -8.0 kcal mol⁻¹ for compounds **3c**, **3e**, **3g**, and **3j**, respectively. Hence, the protein inhibition constants with the studied compounds are 8.75, 5.28, 3.76, and 1.37 μM, respectively, indicating that compound **3j** has the highest affinity for *Klebsiella pneumoniae*, followed by **3g** > **3e** > **3c**.



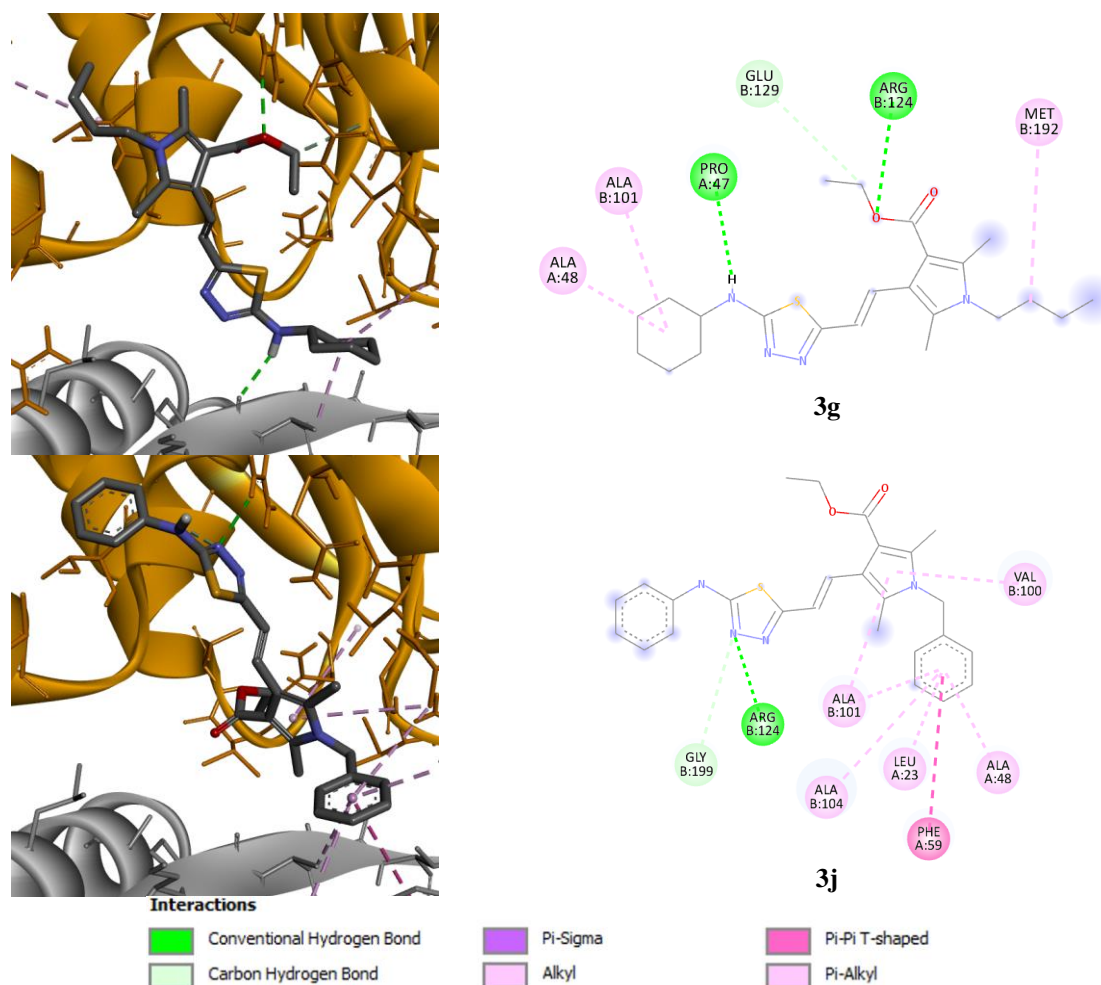


Figure 3. 3D (left) and 2D (right) interactions of compounds **3c, e, g, j** inside the protein's active site. Chain A at the bottom of the figure (grey) and chain B at the top (orange).

The ligand-protein interactions for compounds **3c, e, g, and j** visualised in BIOVIA Discovery Studio Visualizer are shown in Figure 3. Thus, compound **3c** is stabilised within the binding site by four hydrogen bonds with Gly 197, Thr 198, Gly 199, and Cys 200, a weak carbon-hydrogen bond with Gly 71 residue, a π -alkyl and π -sigma interaction between the π -electrons of the thiadiazole ring with Cys 200 and Val 100 respectively, and an alkyl interaction with Val 31 of chain B. It binds to the atoms of chain A by a weak carbon-hydrogen bond with the Met 49 residue and an alkyl interaction with Leu 41.

Compound **3e** forms a hydrogen bond between the oxygen atom of the carboxylate group and Arg 124, a carbon-hydrogen bond with the Glu 129 residue, a π -alkyl interaction of aromatic fragments with Ala 101 and Val 196, and an alkyl interaction of Met 192 of chain B. With chain A, it forms a hydrogen bond between the amino group and Pro 47, and a π -alkyl interaction with Ala 48.

Compound **3g** forms a hydrogen bond between the oxygen atom of the carboxylate group and Arg 124, a carbon-hydrogen bond with Glu 129, and alkyl interactions with Ala 101 and Met 192 of chain B. With chain A, it is stabilized by a hydrogen bond between the amino group and Pro 47 and an alkyl interaction with Ala 48. In general, the binding of compounds **3e** and **3g** occurs to almost the same amino acid residues of the protein. However, compound **3g** lacks interaction via π -electrons of aromatic fragments, which is replaced by π -alkyl interaction.

In compound **3j**, the nitrogen atom of the thiadiazole cycle forms a hydrogen bond with Arg 124 and a carbon-hydrogen bond with Gly 199, a π -alkyl interaction of the pyrrole and

benzyl fragments with Val 100, Ala 101, and Ala 104 of chain B. It is bound to chain A through the benzyl fragment by the π -alkyl interaction of Leu 23 and Ala 48 and the T-shaped π - π interaction with Phe 59.

It should be noted that compounds **3e**, **g**, and **j** are characterised by a significant lipophilic interaction between the A and B chains in the region of Ala 48 and Ala 101, respectively, due to non-polar phenyl, cyclohexenyl, or benzyl groups. The absence of larger non-polar groups in compound **3c** reduces its ability to bind in the lipophilic region between chains A and B, which probably explains its lower binding energy in the protein's active site. In compound **3j**, the presence of a benzyl group facilitates its better interaction in the lipophilic centre of the protein (Figure 3), which can cause its higher binding energy. As shown, in this region of the protein structure, there are no hydrogen bond donors or acceptors, and the benzene ring of Phe 59 is present. The distribution of MESP (Figure 4) shows the presence of positively and negatively charged regions on the amino group, thiadiazole ring, and carboxylate group, making this part of the molecule more polar and hydrophilic. That is why it is located closer to the B chain, which is hydrophilic at the binding site. Also, the presence of a greater number of hydrogen bond donors and acceptors allows the chain to be bonded to them.

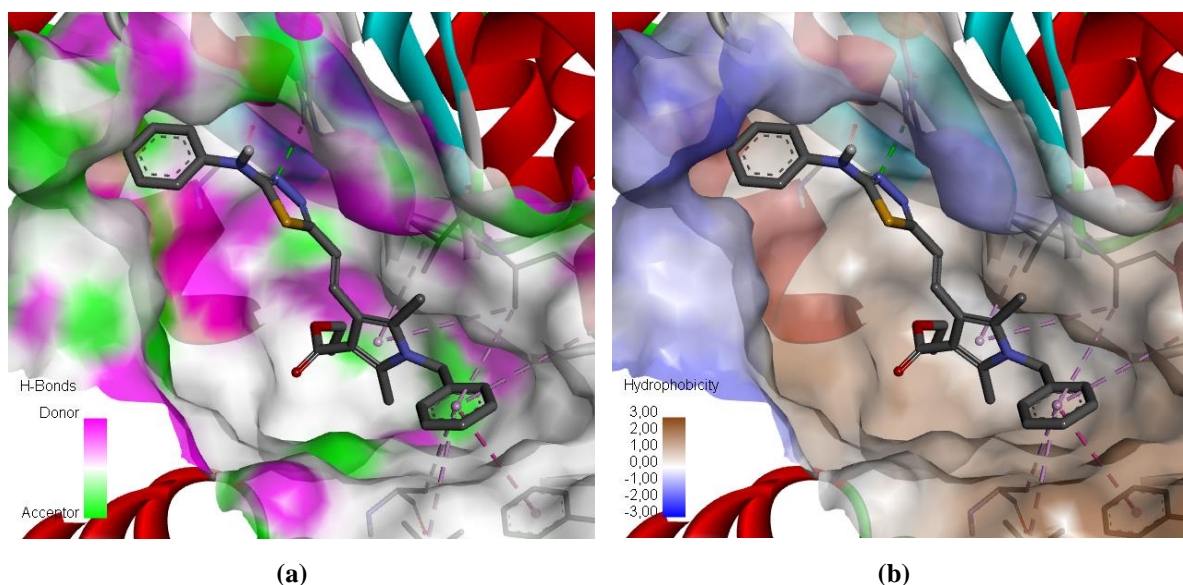


Figure 4. The location of (a) hydrogen bond donors and acceptors; (b) hydrophobic and hydrophilic regions (right) in the active site of protein interaction, and the location of compound 3j in it.

4. Conclusions

A convenient and efficient approach to the synthesis of new heterocyclic ensembles with substituted pyrrole and 1,3,4-thiadiazole cycles has been developed. This approach involves condensing 3-(pyrrole-4-yl)acrylic acids with substituted thiosemicarbazides in boiling POCl_3 . A study of antibacterial activity proves that these compounds are active against the strains *Klebsiella pneumoniae* ATCC 1388 and *Pseudomonas aeruginosa* ATCC 27853. The molecular docking mechanism with the antimicrobial target ThiM from *Klebsiella* was studied using AutoDock Vina for the most active synthesized compounds **3c**, **e**, **g**, and **j**. It was found that a compound **3j** shows the highest affinity to this kinase.

Author Contributions

Conceptualization, M.V. and V.C.; methodology, A.G.; software, D.M and O.M.; validation, D.M and O.M.; formal analysis, D.M., O.M. and S.D.; investigation, S.K., M.F., N.Y. and A.G; resources, S.K., M.F. and V.C.; data curation, V.C and A.G.; writing—original draft preparation, A.G and M.V.; writing—review and editing, S.K. and V.C.; visualization, D.M ; supervision, M.V.; project administration, A.G.. All authors have read and agreed to the published version of the manuscript.

Institutional Review Board Statement

Not applicable.

Informed Consent Statement

Not applicable.

Data Availability Statement

Data supporting the findings of this study are available upon reasonable request from the corresponding author.

Funding

This research received no external funding.

Acknowledgments

We would like to thank Enamine Ltd for the material and technical support, and the “European Chemistry School for Ukrainians” (<https://ecpsfu.org/>) for new scientific ideas.

Conflicts of Interest

The authors disclosed no conflict of interest.

References

1. Bryant, D.A.; Hunter, C.N.; Warren, M.J. Biosynthesis of the modified tetrapyrroles—the pigments of life. *J. Biol. Chem.* **2020**, *295*, 6888–6925, <https://doi.org/10.1074/jbc.REV120.006194>.
2. Wood, J.M.; Furkert, D.P.; Brimble, M.A. 2-Formylpyrrole natural products: origin, structural diversity, bioactivity and synthesis. *Nat. Prod. Rep.* **2019**, *36*, 289-306, <https://doi.org/10.1039/c8np00051d>.
3. Seipp, K.; Geske, L.; Opatz, T. Marine Pyrrole Alkaloids. *Mar. Drugs* **2021**, *19*, 514, <https://doi.org/10.3390/md19090514>.
4. Ferrari, S.M.; Centanni, M.; Virili, C.; Miccoli, M.; Ferrari, P.; Ruffilli, I.; Ragusa, F.; Antonelli, A.; Fallahi, P. Sunitinib in the Treatment of Thyroid Cancer. *Curr. Med. Chem.* **2019**, *26*, 963-972, <https://doi.org/10.2174/0929867324666171006165942>.
5. Anderson, T.J.; Grégoire, J.; Pearson, G.J.; Barry, A.R.; Couture, P.; Dawes, M.; Francis, G.A.; Genest, J.; Grover, S.; Gupta, M.; Hegele, R.A.; Lau, D.C.; Leiter, L.A.; Lonn, E.; Mancini, G.B.J.; McPherson, R.; Ngui, D.; Poirier, P.; Sievenpiper, J.L.; Stone, J.A.; Thanassoulis, G.; Ward, R. 2016 Canadian Cardiovascular Society Guidelines for the Management of Dyslipidemia for the Prevention of Cardiovascular Disease in the Adult. *Can. J. Cardiol.* **2016**, *32*, 1263-1282, <https://doi.org/10.1016/j.cjca.2016.07.510>.
6. Cordrey, L.J. Tolmetin Sodium, a New Anti-Arthritis Drug: Double-Blind and Long-Term Studies. *J. Am. Geriatr. Soc.* **1976**, *24*, 440-446, <https://doi.org/10.1111/j.1532-5415.1976.tb03256.x>.

7. Deutschenbaur, L.; Beck, J.; Kiyhankhadiv, A.; Mühlhauser, M.; Borgwardt, S.; Walter, M.; Hasler, G.; Sollberger, D.; Lang, U.E. Role of calcium, glutamate and NMDA in major depression and therapeutic application. *Prog. Neuro-Psychopharmacol. Biol. Psychiatry* **2016**, *64*, 325-333, <https://doi.org/10.1016/j.pnpbp.2015.02.015>.
8. Demir, A.S.; Akhmedov, I.M.; Sesenoglu, Ö. Synthesis of 1,2,3,5-tetrasubstituted pyrrole derivatives from 2-(2-bromoallyl)-1,3-dicarbonyl compounds. *Tetrahedron* **2002**, *58*, 9793-9799, [https://doi.org/10.1016/s0040-4020\(02\)01298-x](https://doi.org/10.1016/s0040-4020(02)01298-x).
9. Kros, A.; Nolte, R.J.M.; Sommerdijk, N.A.J.M. Conducting Polymers with Confined Dimensions: Track-Etch Membranes for Amperometric Biosensor Applications. *Adv. Mater.* **2002**, *14*, 1779-1782, [https://doi.org/10.1002/1521-4095\(20021203\)14:23<1779::aid-adma1779>3.0.co;2-t](https://doi.org/10.1002/1521-4095(20021203)14:23<1779::aid-adma1779>3.0.co;2-t).
10. Guernion, N.J.L.; Hayes, W. 3- and 3,4-Substituted Pyrroles and Thiophenes and Their Corresponding Polymers - A Review. *Curr. Org. Chem.* **2004**, *8*, 637-651, <http://dx.doi.org/10.2174/1385272043370771>.
11. Tyagi, R.; Yadav, K.; Srivastava, N.; Sagar, R. Applications of Pyrrole and Pyridine-based Heterocycles in Cancer Diagnosis and Treatment. *Curr. Pharm. Des.* **2024**, *30*, 255-277, <https://doi.org/10.2174/0113816128280082231205071504>.
12. Mateev, E.; Georgieva, M.; Zlatkov, A. Pyrrole as an Important Scaffold of Anticancer Drugs: Recent Advances. *J. Pharm. Pharm. Sci.* **2022**, *25*, 24-40, <https://doi.org/10.18433/jpps32417>.
13. Wei, H.; Cao, Y.; Zhao, C.; Shao, Z.; Huo, X.; Pan, J.; Zhuang, R. Design, synthesis, and anticancer evaluation of alkynylated pyrrole derivatives. *Chem. Biol. Drug Des.* **2024**, *103*, e14484, <https://doi.org/10.1111/cbdd.14484>.
14. Mir, R.H.; Mir, P.A.; Mohi-Ud-Din, R.; Sabreen, S.; Maqbool, M.; Shah, A.J.; Shenmar, K.; Raza, S.N.; Pottoo, F.H. A Comprehensive Review on Journey of Pyrrole Scaffold Against Multiple Therapeutic Targets. *Anti-Cancer Agents Med. Chem.* **2022**, *22*, 3291-3303, <https://doi.org/10.2174/1871520622666220613140607>.
15. Ganesh, B.H.; Raj, A.G.; Aruchamy, B.; Nanjan, P.; Drago, C.; Ramani, P. Pyrrole: A Decisive Scaffold for the Development of Therapeutic Agents and Structure-Activity Relationship. *ChemMedChem* **2024**, *19*, e202300447, <https://doi.org/10.1002/cmdc.202300447>.
16. Faleye, O.S.; Boya, B.R.; Lee, J.-H.; Choi, I.; Lee, J. Halogenated Antimicrobial Agents to Combat Drug-Resistant Pathogens. *Pharmacol. Rev.* **2024**, *76*, 90-141, <https://doi.org/10.1124/pharmrev.123.000863>.
17. Hilmy, K.M.H.; Kishk, F.N.M.; Shahen, E.B.A.; Sobh, E.A.; Hawata, M.A. New pyrrole derivatives as DNA gyrase and 14 α -demethylase inhibitors: Design, synthesis, antimicrobial evaluation, and molecular docking. *Drug Dev. Res.* **2023**, *84*, 1204-1230, <https://doi.org/10.1002/ddr.22080>.
18. Ahmed, S.; Mital, A.; Akhir, A.; Saxena, D.; Ahmad, M.N.; Dasgupta, A.; Chopra, S.; Jain, R. Pyrrole-thiazolidinone hybrids as a new structural class of broad-spectrum anti-infectives. *Eur. J. Med. Chem.* **2023**, *260*, 115757, <https://doi.org/10.1016/j.ejmech.2023.115757>.
19. Karadayi, F.Z.; Başaran, R.; Kişla, M.M.; Eke, B.; Alagöz, Z. Synthesis, antioxidant activity, molecular docking and ADME studies of novel pyrrolebenzimidazole derivatives. *Turk. J. Chem.* **2022**, *46*, 890-902, <https://doi.org/10.55730/1300-0527.3377>.
20. Fortuna, C.G.; Barresi, V.; Bonaccorso, C.; Consiglio, G.; Failla, S.; Trovato-Salinaro, A.; Musumarra, G. Design, synthesis and invitro antitumour activity of new heteroaryl ethylenes. *Eur. J. Med. Chem.* **2012**, *47*, 221-227, <https://doi.org/10.1016/j.ejmech.2011.10.060>.
21. Ballistreri, F.P.; Barresi, V.; Benedetti, P.; Caltabiano, G.; Fortuna, C.G.; Longo, M.L.; Musumarra, G. Design, synthesis and in vitro antitumor activity of new *trans* 2-[2-(heteroaryl)vinyl]-1,3-dimethylimidazolium iodides. *Bioorg. Med. Chem.* **2004**, *12*, 1689-1695, <https://doi.org/10.1016/j.bmc.2004.01.018>.
22. Santhosh, P.; Bugga, S. Androgen receptor antagonists. WO Patent Number 152731 A1, date of patent August 08, **2019**.
23. Sprague, R.H. Cyanine Dyes. I. Absorption of Cyanines Derived from Pyranothiazole and Thiopyranothiazoles. *J. Am. Chem. Soc.* **1957**, *79*, 2275-2281, <https://doi.org/10.1021/ja01566a069>.
24. Biagini, P.; Abbotto, A.; Manfredi, N. Organic dye for a dye sensitized solar cell. Patent Number US 9865403 B2, date of patent January 09, **2018**.
25. Beverina, L.; Fu, J.; Leclercq, A.; Zojer, E.; Pacher, P.; Barlow, S.; Van Stryland, E.W.; Hagan, D.J.; Brédas, J.-L.; Marder, S.R. Two-Photon Absorption at Telecommunications Wavelengths in a Dipolar Chromophore with a Pyrrole Auxiliary Donor and Thiazole Auxiliary Acceptor. *J. Am. Chem. Soc.* **2005**, *127*, 7282-7283, <https://doi.org/10.1021/ja0506881>.

26. Beverina, L.; Crippa, M.; Landenna, M.; Ruffo, R.; Salice, P.; Silvestri, F.; Versari, S.; Villa, A.; Ciaffoni, L.; Collini, E.; Ferrante, C.; Bradamante, S.; Mari, C.M.; Bozio, R.; Pagani, G.A. Assessment of Water-Soluble π -Extended Squaraines as One- and Two-Photon Singlet Oxygen Photosensitizers: Design, Synthesis, and Characterization. *J. Am. Chem. Soc.* **2008**, *130*, 1894-1902, <https://doi.org/10.1021/ja075933a>.
27. Ansteatt, S.; Meares, A.; Ptaszek, M. Amphiphilic Near-IR-Emitting 3,5-Bis(2-Pyrrolylethenyl)BODIPY Derivatives: Synthesis, Characterization, and Comparison with Other (Hetero)Arylethenyl-Substituted BODIPYs. *J. Org. Chem.* **2021**, *86*, 8755-8765, <https://doi.org/10.1021/acs.joc.1c00586>.
28. Coelho, P.J.; Castro, M.C.R.; Raposo, M.M.M. Fast (hetero)aryl-benzothiazolium ethenes photoswitches activated by visible-light at room temperature. *Dyes Pigments* **2015**, *117*, 163-169, <https://doi.org/10.1016/j.dyepig.2015.02.015>.
29. Yamamoto, Y.; Kimachi, T.; Kanaoka, Y.; Kato, S.; Bessho, K.; Matsumoto, T.; Kusakabe, T.; Sugiura, Y. Synthesis and DNA binding properties of amide bond-modified analogues related to distamycin. *Tetrahedron Lett.* **1996**, *37*, 7801-7804, [https://doi.org/10.1016/0040-4039\(96\)01782-0](https://doi.org/10.1016/0040-4039(96)01782-0).
30. Rajeswari, S.; Adesomoju, A.A.; Cava, M.P. Synthesis of new gramine-type analogs of CC-1065. *J. Heterocycl. Chem.* **1989**, *26*, 557-564, <https://doi.org/10.1002/jhet.5570260307>.
31. Anthony, N.G.; Breen, D.; Donoghue, G.; Khalaf, A.I.; Mackay, S.P.; Parkinson, J.A.; Suckling, C.J. A new synthesis of alkene-containing minor-groove binders and essential hydrogen bonding in binding to DNA and in antibacterial activity. *Org. Biomol. Chem.* **2009**, *7*, 1843-1850, <https://doi.org/10.1039/b901898k>.
32. Anthony, N.G.; Breen, D.; Clarke, J.; Donoghue, G.; Drummond, A.J.; Ellis, E.M.; Gemmell, C.G.; Helesbeux, J.-J.; Hunter, I.S.; Khalaf, A.I.; Mackay, S.P.; Parkinson, J.A.; Suckling, C.J.; Waigh, R.D. Antimicrobial Lexitropsins Containing Amide, Amidine, and Alkene Linking Groups. *J. Med. Chem.* **2007**, *50*, 6116-6125, <https://doi.org/10.1021/jm070831g>.
33. Rawal, V.H.; Cava, M.P. Photocyclization of pyrrole analogues of stilbene: an expedient approach to antitumor agent CC-1065. *J. Chem. Soc., Chem. Commun.* **1984**, 1526-1527, <https://doi.org/10.1039/c39840001526>.
34. Hinz, W.; Jones, R.A.; Anderson, T. Pyrrole Studies; 34¹. Synthesis of 1,2-Di(2-pyrrolyl)ethenes and Related Compounds. *Synthesis* **1986**, *8*, 620-623, <https://doi.org/10.1055/s-1986-31722>.
35. Matysiak, J. Biological and Pharmacological Activities of 1,3,4-Thiadiazole Based Compounds. *Mini Rev. Med. Chem.* **2015**, *15*, 762-775, <https://doi.org/10.2174/1389557515666150519104057>.
36. Haider, S.; Alam, M.S.; Hamid, H. 1,3,4-Thiadiazoles: A potent multi targeted pharmacological scaffold. *Eur. J. Med. Chem.* **2015**, *92*, 156-177, <https://doi.org/10.1016/j.ejmech.2014.12.035>.
37. Stecoza, C.E.; Nitulescu, G.M.; Draghici, C.; Caproiu, M.T.; Hanganu, A.; Oлару, O.T.; Mihai, D.P.; Bostan, M.; Mihaila, M. Synthesis of 1,3,4-Thiadiazole Derivatives and Their Anticancer Evaluation. *Int. J. Mol. Sci.* **2023**, *24*, 17476, <https://doi.org/10.3390/ijms242417476>.
38. Yurttas, L.; Evren, A.E.; AlChaib, H.; Temel, H.E.; Çiftçi, G.A. Synthesis, molecular docking, and molecular dynamic simulation studies of new 1,3,4-thiadiazole derivatives as potential apoptosis inducers in A549 lung cancer cell line. *J. Biomol. Struct. Dyn.* **2025**, *43*, 3814-3829, <https://doi.org/10.1080/07391102.2023.2300125>.
39. Shulgau, Z.; Palamarchuk, I.V.; Sergazy, S.; Urazbayeva, A.; Ramankulov, Y.; Kulakov, I.V. Synthesis, Computational Study, and In Vitro α -Glucosidase Inhibitory Action of 1,3,4-Thiadiazole Derivatives of 3-Aminopyridin-2(1H)-ones. *Pharmaceuticals* **2024**, *17*, 377, <https://doi.org/10.3390/ph17030377>.
40. Shirato, S.; Kagaya, F.; Suzuki, Y.; Joukou, S. Stevens-Johnson Syndrome Induced by Methazolamide Treatment. *Arch. Ophthalmol.* **1997**, *115*, 550-553, <https://doi.org/10.1001/archophth.1997.01100150552021>.
41. Enanga, B.; Ariyanayagam, M.R.; Stewart, M.L.; Barrett, M.P. Activity of Megazol, a Trypanocidal Nitroimidazole, Is Associated with DNA Damage. *Antimicrob. Agents Chemother.* **2003**, *47*, 3368-3370, <https://doi.org/10.1128/AAC.47.10.3368-3370.2003>.
42. Kemsykyi, S.; Fedoriv, M.; Palamar, A.; Grozav, A.; Chornous, V.; Kutsyk, R.; Dorokhov, V.; Vovk, M. Synthesis and evaluation of antimicrobial activity of some new 3-(pyrrol-4-yl)acrylamide derivatives. *Curr. Chem. Lett.* **2023**, *12*, 519-528, <https://doi.org/10.5267/j.ccl.2023.3.004>.
43. Kowalska-Krochmal, B.; Dudek-Wicher, R. The Minimum Inhibitory Concentration of Antibiotics: Methods, Interpretation, Clinical Relevance. *Pathogens* **2021**, *10*, 165, <https://doi.org/10.3390/pathogens10020165>.

44. Nazarchuk, O.A. Antiseptics: modern strategy of struggle with causing agents of the infection complications. *Klin. Khir.* **2016**, *9*, 59-61.
45. Crowley, P.D.; Gallagher, H.C. Clotrimazole as a pharmaceutical: past, present and future. *J. Appl. Microbiol.* **2014**, *117*, 611-617, <https://doi.org/10.1111/jam.12554>.
46. Firsch, M.J.; Trucks, G.W.; Schlegel, H.B.; Scuseria, G.E.; Robb, M.A.; Cheeseman, J.R.; Scalmani, G.; Barone, V.; Petersson, G.A.; Nakatsuji, H.; Li, X.; Caricato, M.; Marenich, A.; Bloino, J.; Janesko, B.G.; Gomperts, R.; Mennucci, B.; Hratchian, H.P.; Ortiz, J.V.; Izmaylov, A.F.; Sonnenberg, J.L.; Williams-Young, D.; Ding, F.; Lipparini, F.; Egidi, F.; Goings, J.; Peng, B.; Petrone, A.; Henderson, T.; Ranasinghe, D.; Zakrzewski, V.G.; Gao, J.; Rega, N.; Zheng, G.; Liang, W.; Hada, M.; Ehara, M.; Toyota, K.; Fukuda, R.; Hasegawa, J.; Ishida, M.; Nakajima, T.; Honda, Y.; Kitao, O.; Nakai, H.; Vreven, T.; Throssell, K.; Montgomery Jr., J.A.; Peralta, J.E.; Ogliaro, F.; Bearpark, M.; Heyd, J.J.; Brothers, E.; Kudin, K.N.; Staroverov, V.N.; Keith, T.; Kobayashi, R.; Normand, J.; Raghavachari, K.; Rendell, A.; Burant, J.C.; Iyengar, S.S.; Tomasi, J.; Cossi, M.; Millam, J.M.; Klene, M.; Adamo, C.; Cammi, R.; Ochterski, J.W.; Martin, R.L.; Morokuma, K.; Farkas, O.; Foresman, J.B.; Fox, D.J. Gaussian, Inc., Wallingford CT, **2016**.
47. Gázquez, J.L.; Cedillo, A.; Vela, A. Electrodonating and Electroaccepting Powers. *J. Phys. Chem. A* **2007**, *111*, 1966-1970, <https://doi.org/10.1021/jp065459f>.
48. Trott, O.; Olson, A.J. AutoDock Vina: Improving the speed and accuracy of docking with a new scoring function, efficient optimization, and multithreading. *J. Comput. Chem.* **2010**, *31*, 455-461, <https://doi.org/10.1002/jcc.21334>.
49. Buchini, S.; Buschiazzo, A.; Withers, S.G. A New Generation of Specific *Trypanosoma cruzi* trans-Sialidase Inhibitors. *Angew. Chem. Int. Ed.* **2008**, *47*, 2700-2703, <https://doi.org/10.1002/anie.200705435>.
50. Leite, A.C.L.; de M. Moreira, D.R.; de O. Cardoso, M.V.; Hernandez, M.Z.; Alves Pereira, V.R.; Silva, R.O.; Kiperstok, A.C.; da S. Lima, M.; Soares, M.B.P. Synthesis, Cruzain Docking, and in vitro Studies of Aryl-4-Oxothiazolyldrazones Against *Trypanosoma cruzi*. *ChemMedChem* **2007**, *2*, 1339-1345, <https://doi.org/10.1002/cmdc.200700022>.
51. Sayiner, H.S.; Yilmazer, M.I.; Abdelsalam, A.T.; Ganim, M.A.; Baloglu, C.; Altunoglu, Y.C.; Gür, M.; Saracoglu, M.; Attia, M.S.; Mahmoud, S.A.; Mohamed, E.H.; Boukherroub, R.; Al-Shaalan, N.H.; Alharthi, S.; Kandemirli, F.; Amin, M.A. Synthesis and characterization of new 1,3,4-thiadiazole derivatives: study of their antibacterial activity and CT-DNA binding. *RSC Adv.* **2022**, *12*, 29627-29639, <https://doi.org/10.1039/D2RA02435G>.
52. Micheli, F.; Bernardelli, A.; Bianchi, F.; Braggio, S.; Castelletti, L.; Cavallini, P.; Cavanni, P.; Cremonesi, S.; Cin, M.D.; Feriani, A.; Oliosi, B.; Semeraro, T.; Tarsi, L.; Tomelleri, S.; Wong, A.; Visentini, F.; Zonzini, L.; Heidbreder, C. 1,2,4-Triazolyl octahydropyrrolo[2,3-*b*]pyrroles: A new series of potent and selective dopamine D3 receptor antagonists. *Bioorg. Med. Chem.* **2016**, *24*, 1619-1636, <https://doi.org/10.1016/j.bmc.2016.02.031>.
53. Khanfar, M.A.; Reiner, D.; Hagenow, S.; Stark, H. Design, synthesis, and biological evaluation of novel oxadiazole- and thiazole-based histamine H₃R ligands. *Bioorg. Med. Chem.* **2018**, *26*, 4034-4046, <https://doi.org/10.1016/j.bmc.2018.06.028>.
54. Teknikel, Ö.Ç.; Öğütçü, H.; Doyduk, D.; Dişli A. Synthesis and antimicrobial activities of unsymmetrical thioditrazoles and their precursor thiotetrazoles. *Org. Commun.* **2023**, *16*, 204-211, <https://doi.org/10.25135/acg.oc.158.2309.2893>.
55. Stojowska-Swędryńska, K.; Łupkowska, A.; Kuczyńska-Wisnik, D.; Laskowska, E. Antibiotic Heteroresistance in *Klebsiella pneumoniae*. *Int. J. Mol. Sci.* **2022**, *23*, 449, <https://doi.org/10.3390/ijms23010449>.
56. El-Sheshtawy, H.S.; Ibrahim, M.M.; El-Mehasseb, I.; El-Kemary, M. Orthogonal hydrogen/halogen bonding in 1-(2-methoxyphenyl)-1H-imidazole-2(3H)-thione-I₂ adduct: An experimental and theoretical study. *Spectrochim. Acta - A: Mol. Biomol. Spectrosc.* **2015**, *143*, 120-127, <https://doi.org/10.1016/j.saa.2015.02.043>.
57. Murray, J.S.; Politzer, P. The electrostatic potential: an overview. *WIREs Comput. Mol. Sci.* **2011**, *1*, 153-163, <https://doi.org/10.1002/wcms.19>.

Publisher's Note & Disclaimer

The statements, opinions, and data presented in this publication are solely those of the individual author(s) and contributor(s) and do not necessarily reflect the views of the publisher and/or the editor(s). The publisher and/or

the editor(s) disclaim any responsibility for the accuracy, completeness, or reliability of the content. Neither the publisher nor the editor(s) assume any legal liability for any errors, omissions, or consequences arising from the use of the information presented in this publication. Furthermore, the publisher and/or the editor(s) disclaim any liability for any injury, damage, or loss to persons or property that may result from the use of any ideas, methods, instructions, or products mentioned in the content. Readers are encouraged to independently verify any information before relying on it, and the publisher assumes no responsibility for any consequences arising from the use of materials contained in this publication.